

# Minimal model for transient swimming in a liquid crystal

Madison S. Krieger,<sup>1</sup> Marcelo A. Dias,<sup>2,3</sup> and Thomas R. Powers<sup>1,4</sup>

<sup>1</sup>*School of Engineering, Brown University, Providence, RI 02912, USA*

<sup>2</sup>*Aalto Science Institute (ASCI), Aalto University, Otaniementie 17, FI-02150 Espoo, Finland*

<sup>3</sup>*NORDITA, Roslagstullsbacken 23, 106 92 Stockholm, Sweden*

<sup>4</sup>*Department of Physics, Brown University, Providence, RI 02192, USA*

(Dated: Submitted June 4, 2015)

When a microorganism begins swimming from rest in a Newtonian fluid such as water, it rapidly attains its steady-state swimming speed since changes in the velocity field spread quickly when the Reynolds number is small. However, swimming microorganisms are commonly found or studied in complex fluids. Because these fluids have long relaxation times, the time to attain the steady-state swimming speed can also be long. In this article we study the swimming startup problem in the simplest liquid crystalline fluid: a two-dimensional hexatic liquid crystal film. We study the dependence of startup time on anchoring strength and Ericksen number, which is the ratio of viscous to elastic stresses. For strong anchoring, the fluid flow starts up immediately but the liquid crystal field and swimming velocity attain their sinusoidal steady-state values after a time proportional to the relaxation time of the liquid crystal. When the Ericksen number is high, the behavior is the same as in the strong anchoring case for any anchoring strength. We also find that the startup time increases with the ratio of the rotational viscosity to the shear viscosity, and then ultimately saturates once the rotational viscosity is much greater than the shear viscosity.

## I. INTRODUCTION

The hydrodynamics of natural and artificial microscopic swimmers in Newtonian and complex fluids continues to be an active area of research [1–5]. Many of these studies focus on steady-state swimming. However, natural swimmers start, stop, and change direction, and artificial swimmers must do the same to be of use. Therefore, it is of interest to study transient swimming problems, such as the acceleration of a swimmer from rest. In a Newtonian fluid of viscosity  $\mu$  and density  $\rho$ , the relevant time scale  $t_v$  (‘v’ for ‘viscous’) for the startup of flow is the time  $t_v = \rho/(\mu q^2)$  for changes in velocity to spread over a distance of order  $1/q$ . For water and a length scale  $1/q \approx 1 \mu\text{m}$ , we have  $t_v \approx 1 \mu\text{s}$ , which is much shorter than the characteristic beat or rotation frequency of swimming microorganisms, such as 0.001 s for *Vibrio alginolyticus* [6], 0.01 s for *Escherichia coli* [7], 0.02 s for *Chlamydomonas reinhardtii* [8] and sea urchin sperm [9], 0.05 s for human sperm [10], and 0.5 s for *Caenorhabditis elegans* [11]. Calculations for how the swimming speed rapidly rises to its steady state value for an idealized swimmer in a Newtonian fluid were presented by Pak and Lauga [12]. Complex fluids have additional time scales, which are much longer than  $t_v$ , and can be comparable to or even longer than the characteristic beat period. For example, polymer solutions in which swimming has been studied can have relaxation times of the order of seconds [11, 13]. Likewise, the airway mucus encountered by beating cilia has relaxation times of the order of tens of seconds [14, 15]. The startup problem for a swimmer in a viscoelastic fluid has been examined by Elfring and Lauga [16]. Swimming bacteria have also been recently studied in liquid crystal solutions [17, 18]. For a liquid crystal with Franck elastic constant  $K \approx 10 \text{ pN}$ , and shear viscosity  $\mu \approx 10 \text{ Pa-s}$  [17], the characteris-

tic relaxation time  $t_e$  (‘e’ for ‘elastic’) for distortions of the liquid crystal with length scale  $1/q \approx 1 \mu\text{m}$  is  $t_e = \mu/(Kq^2) \approx 10 \text{ s}$ . The long relaxation times of these complex fluids can lead to much longer-lived transient swimming flows than in the Newtonian case.

In this article we study the startup problem for an idealized swimmer with small amplitude waves in a hexatic liquid crystal film. The hexatic phase is studied because its theory is mathematically simpler than that of the nematic phase, yet it retains some of the same distinctive features such as Franck elasticity, rotational viscosity, and anchoring effects. We show that the time required to attain the steady swimming speed is proportional to the relaxation time of the liquid crystal. Since this time is much longer than the viscous startup time  $t_v$ , the swimmer first attains the Newtonian swimming speed in a time comparable to  $t_v$ , and then reaches the final swimming speed over a longer time  $t_e$ . We study how the evolution of the swimming velocity depends on the anchoring strength of the the liquid crystal at the surface of the swimmer, and also the Ericksen number  $Er$ , which is the ratio of viscous to elastic stresses. For strong anchoring, we find that the swimming speed reaches its ultimate value after a time proportional to the Ericksen number. At high Ericksen number, the behavior of the flow field, the liquid crystal configuration, and the swimming speed is independent of anchoring strength, and is given by the strong anchoring case. When the anchoring strength vanishes, we find that the swimming speed can oscillate as it approaches its final value, and that the swimmer can even reverse direction several times before reaching its steady speed.

The outline of the paper is as follows. Section II describes the governing equations and timescales. Then the case of strong anchoring is solved analytically in Sec. III. Section IV considers the case of arbitrary an-

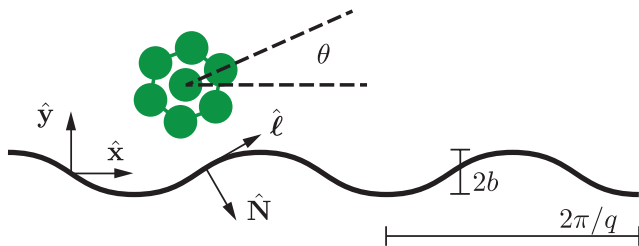


Figure 1. (Color online) Sketch of the one-dimensional swimmer and definition of the angle field  $\theta$ . The liquid crystal particles are not drawn to scale. The outward pointing unit normal vector on the swimmer is  $\hat{\mathbf{N}}$ , and the tangent vector to the swimmer is  $\hat{\ell}$ .

choring strength in the limits of high and low Ericksen number, paying special attention to the striking case of zero anchoring strength. The conclusion is Sec. V.

## II. SETUP AND GOVERNING EQUATIONS

### A. The swimmer

The swimmer is a line with a prescribed traveling wave. In the frame of the swimmer, the material points on the swimmer have coordinates

$$x_m = x \quad (1)$$

$$y_m = b \sin[qx - \omega(t)t], \quad (2)$$

where  $b$  is the amplitude of the wave,  $q$  is the wavenumber, and  $\omega(t)$  is the time-dependent frequency (Fig. 1). Following Taylor [19], we assume the amplitude is small compared to the wavelength,  $b^2 q^2 \ll 1$ . Initially, the frequency vanishes,  $\omega(0) = 0$ , and the fluid is motionless. The frequency rises to its final value  $\omega_\infty$  with a characteristic time scale  $t_s$  ('s' for swimmer). This characteristic time is long compared to the viscous startup time  $t_v$ , but seems to be comparable to or longer than the beat period  $2\pi/\omega_\infty$ , depending on the species. For example, the switching time from backward to forward swimming, or vice versa, in *V. alginolyticus* is of the order of tenths of seconds [20], about ten times longer than the beat period. When sea urchin spermatozoa are rendered immotile by lowering the pH, the waveform takes a few periods to restart once the pH is raised again [21].

### B. Hexatic Liquid Crystals

The swimmer lies in a two-dimensional hexatic liquid crystal. Recall that a hexatic liquid crystal has six-fold bond-orientational order, described by an angle field  $\theta$ , where  $\theta$  and  $\theta + 2\pi/6$  denote the same physical configuration [22] (Fig. 1). We use the notation and conventions of reference [23], and refer the reader there for more details on the derivation of the governing equations. We

consider incompressible flow,  $\nabla \cdot \mathbf{v} = 0$ , where  $\mathbf{v}$  is the velocity. The dynamical equations for velocity and angle field are

$$-\nabla p + \mu \nabla^2 \mathbf{v} - K(\nabla \theta) \nabla^2 \theta + \frac{K}{2} \nabla \times (\hat{\mathbf{z}} \nabla^2 \theta) = \mathbf{0} \quad (3)$$

$$\partial_t \theta + \mathbf{v} \cdot \nabla \theta - \frac{1}{2} \hat{\mathbf{z}} \cdot \nabla \times \mathbf{v} = \frac{K}{\gamma} \nabla^2 \theta, \quad (4)$$

where  $\mu$  is shear viscosity,  $K$  is the Frank elastic constant,  $\hat{\mathbf{z}}$  is the unit vector perpendicular to the plane of the liquid crystal film, and  $\gamma$  is the rotational viscosity [24]. Note that the pressure  $p$  has been defined so that it vanishes in equilibrium [23]; in other words,  $p$  is the actual pressure minus the equilibrium pressure arising from Frank elasticity [22]. Note also that we have assumed the Reynolds number to be vanishingly small. This approximation is valid because the liquid crystal solutions which motivate our study are 10000 times as viscous as water [17], and also because we do not attempt to resolve the dynamics on the scale  $t_v$ .

At the swimmer, we assume no-slip boundary conditions on the velocity field:

$$\mathbf{v}(x_m, y_m, t) = \dot{y}_m \hat{\mathbf{y}}. \quad (5)$$

Far from the swimmer, the velocity field has an unknown uniform value  $\mathbf{v}(y \rightarrow \infty) = U \hat{\mathbf{x}}$  that we must solve for. The flow  $U$  in the rest frame is the swimming velocity in the lab frame, which has opposite sign to  $U$ . We also impose anchoring conditions on the liquid crystal near the swimmer surface. Since we assume the swimmer has a small slope, we may assume the angle  $\phi$  between the swimmer tangent vector  $\hat{\ell}$  and the  $x$ -axis is small. With accuracy of order  $b^2 q^2$ , the anchoring condition becomes [23]

$$K \hat{\mathbf{N}} \cdot \nabla \theta + W(\theta - \phi) = 0, \quad (6)$$

where  $\hat{\mathbf{N}}$  is the outward-pointing normal vector and  $W$  is an energy per unit length giving the strength of the anchoring potential.

As mentioned earlier, the initial condition for the fluid is  $\mathbf{v} = \mathbf{0}$ . The initial condition for the angle field is the equilibrium configuration, which satisfies  $\nabla^2 \theta = 0$  and the anchoring condition Eq. (6).

### C. Time scales, nondimensionalization, and the impulsive startup problem

There are four time scales in our problem, with a strong separation of the viscous time scale from the others:

$$t_v \ll \omega_\infty^{-1} < t_s < t_e. \quad (7)$$

To make the governing equations dimensionless, we use  $1/\omega_\infty$  as the units of time and  $1/q$  as the units of length.

Then, with  $p$  measured in units of  $\mu\omega_\infty$ , we have [23]

$$-\nabla p + \nabla^2 \mathbf{v} - \frac{1}{\text{Er}} \nabla \theta (\nabla^2 \theta) + \frac{1}{2\text{Er}} \nabla \nabla^2 \theta \times \hat{\mathbf{z}} = 0 \quad (8)$$

$$\partial_t \theta + \mathbf{v} \cdot \nabla \theta - \frac{1}{2} \hat{\mathbf{z}} \cdot \nabla \times \mathbf{v} - \frac{\mu}{\gamma} \frac{1}{\text{Er}} \nabla^2 \theta = 0, \quad (9)$$

where

$$\text{Er} = \frac{\mu\omega_\infty}{Kq^2}. \quad (10)$$

It is convenient to use the stream function  $\psi$ , which automatically enforces the constraint of incompressibility by the definition  $\mathbf{v} = \nabla \times (\psi \hat{\mathbf{z}})$ . In terms of  $\psi$ , the governing equations are

$$\nabla^4 \psi + \frac{1}{2\text{Er}} \nabla^4 \theta + \frac{1}{\text{Er}} \hat{\mathbf{z}} \cdot \nabla \theta \times \nabla \nabla^2 \theta = 0 \quad (11)$$

$$\partial_t \theta + \frac{1}{2} \nabla^2 \psi + \hat{\mathbf{z}} \cdot \nabla \theta \times \nabla \psi - \frac{\mu}{\gamma} \frac{1}{\text{Er}} \nabla^2 \theta = 0. \quad (12)$$

In dimensionless form, the boundary condition for the angle field  $\theta(x_m, y_m)$  at the swimmer is

$$\hat{\mathbf{N}} \cdot \nabla \theta + w(\theta - \phi) = 0, \quad (13)$$

where  $w = W/(Kq)$ . The dimensionless no-slip boundary condition at  $(x_m, y_m)$  is

$$\mathbf{v}(x_m, y_m) = -\epsilon \frac{d[\omega(t)t]}{dt} \cos[x - \omega(t)t] \hat{\mathbf{y}}, \quad (14)$$

where we have introduced  $\epsilon = bq$ . Note that we are also measuring frequency in units of  $\omega_\infty$ . To simplify the analysis, we will consider the impulsive startup problem and suppose that  $\omega_\infty \tau \ll 1$ , even though  $\tau$  is typically a longer time scale than  $1/\omega_\infty$ . Therefore, we suppose the dimensionless frequency impulsively jumps from zero to unity at  $t = 0$ . Denoting by  $H(t)$  the unit Heaviside step function, we have

$$\mathbf{v}(x_m, y_m) = -\epsilon \frac{d[H(t)t]}{dt} \cos[x - H(t)t] \hat{\mathbf{y}}. \quad (15)$$

Our task is to solve for the swimming speed  $-U$  as a function of time. We expand in powers of  $\epsilon$ ,

$$\mathbf{v} = \mathbf{v}^{(1)} + \mathbf{v}^{(2)} + \dots \quad (16)$$

$$\theta = \theta^{(1)} + \theta^{(2)} + \dots \quad (17)$$

where the superscript denotes the power of  $\epsilon$ .

### III. STRONG ANCHORING

First we consider the case of strong anchoring,  $w \rightarrow \infty$ , since in this limit we can get explicit expressions for  $\theta$  and  $U$  as functions of time for impulsive startup of the beating.

In terms of the stream function, the first-order parts

of equations (11–12) are

$$\nabla^4 \psi^{(1)} + \frac{1}{2\text{Er}} \nabla^4 \theta^{(1)} = 0 \quad (18)$$

$$\partial_t \theta^{(1)} + \frac{1}{2} \nabla^2 \psi^{(1)} - \frac{\mu}{\gamma \text{Er}} \nabla^2 \theta^{(1)} = 0. \quad (19)$$

The initial conditions are

$$\theta^{(1)}(x, y, t = 0) = \epsilon e^{-y} \cos x \quad (20)$$

$$\psi^{(1)}(x, y, t = 0) = 0, \quad (21)$$

and the boundary conditions are

$$\nabla \psi^{(1)}|_{y=0} = -\epsilon \frac{d}{dt} \sin[x - tH(t)] \hat{\mathbf{x}} \quad (22)$$

$$\theta^{(1)}|_{y=0} = \epsilon \cos(x - t). \quad (23)$$

Note that the angle field has some initial distortion due to the strong-anchoring condition. Furthermore, the initial condition for the angle field has exactly the same spatial form as the sinusoidal-steady state solution for  $\theta^{(1)}$  that was found in [23]. Thus, there is no need for distortions in the angle-field to spread once the swimmer waveform starts up; the angle field simply starts to oscillate in time with the same frequency as the swimmer waveform. The fluid velocity, however, changes discontinuously, since we do not resolve dynamics on the small timescale  $t_v$  (studied in [12]). For  $t > 0$ , we find

$$v_x^{(1)} = -\epsilon y e^{-y} \sin(x - t) \quad (24)$$

$$v_y^{(1)} = -\epsilon(1 + y)e^{-y} \cos(x - t) \quad (25)$$

$$\theta^{(1)} = \epsilon e^{-y} \cos(x - t). \quad (26)$$

These results can also be found by directly solving the equations (18–19) using Laplace transforms.

To see how the final sinusoidal steady-state solution emerges, we must turn to the second-order equations:

$$\begin{aligned} & -\nabla p^{(2)} + \nabla^2 \mathbf{v}^{(2)} \\ & = -\frac{1}{\text{Er}} \left[ \frac{1}{2} \nabla \times (\hat{\mathbf{z}} \nabla^2 \theta^{(2)}) - \nabla \theta^{(1)} \nabla^2 \theta^{(1)} \right], \end{aligned} \quad (27)$$

and

$$\frac{1}{\text{Er}} \frac{\mu}{\gamma} \nabla^2 \theta^{(2)} = \partial_t \theta^{(2)} + \mathbf{v}^{(1)} \cdot \nabla \theta^{(1)} - \frac{1}{2} \hat{\mathbf{z}} \cdot \nabla \times \mathbf{v}^{(2)}. \quad (28)$$

Averaging over a spatial wavelength, these equations become

$$\partial_y^2 \langle v_x^{(2)} \rangle + \frac{1}{2\text{Er}} \partial_y^3 \langle \theta^{(2)} \rangle = f \quad (29)$$

$$\partial_t \langle \theta^{(2)} \rangle = \frac{1}{\text{Er}} \frac{\mu}{\gamma} \partial_y^2 \langle \theta^{(2)} \rangle - \frac{1}{2} \langle \partial_y v_x^{(2)} \rangle - g, \quad (30)$$

where  $f = \langle \partial_x \theta^{(1)} \nabla^2 \theta^{(1)} \rangle / \text{Er}$  and  $g \equiv \langle \mathbf{v}^{(1)} \cdot \nabla \theta^{(1)} \rangle$ . For

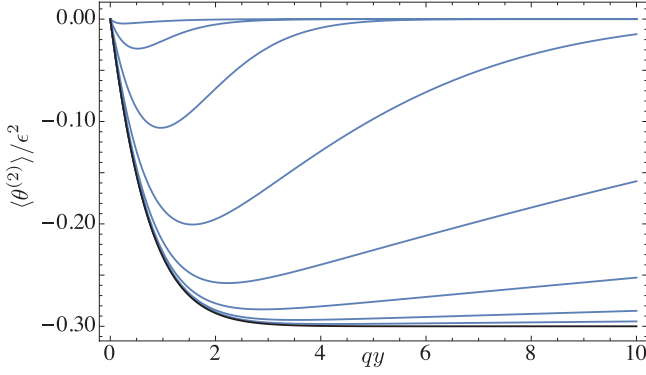


Figure 2. (Color online) Time evolution of the average second-order angle field  $\langle \theta^{(2)} \rangle$  for  $Er = 1$  and  $\mu = \gamma$ , or  $D = 5/4$ . Starting from the top of the figure, the first eight curves (blue) correspond to  $\omega_\infty t = 10^{-2}, 10^1, \dots, 10^5$ , and the last curve (black) corresponds to the steady-state value, or  $\omega_\infty t \rightarrow \infty$ .

strong anchoring,

$$f = 0 \quad (31)$$

$$g = (\epsilon^2/2)(1 + 2y) \exp(-2y)H(t). \quad (32)$$

The initial conditions are  $\langle \theta^{(2)} \rangle|_{t=0} = 0$  and  $\langle \mathbf{v}^{(2)} \rangle|_{t=0} = 0$ , and the boundary conditions are

$$\langle v_x^{(2)} \rangle|_{y=0} = -\langle y_m \partial_y v_x^{(1)} \rangle|_{y=0} = \epsilon^2/2 \quad (33)$$

$$\langle \theta^{(2)} \rangle|_{y=0} = 0. \quad (34)$$

Note that to arrive at (33–34), we expanded the boundary condition at  $y = y_m$  and used the fact that the strong-anchoring angle field is out of phase with the wave  $y = y_m$ .

Using  $\mathcal{L}$  to denote the Laplace transform,

$$\mathcal{L}\{f(t)\} = \int_0^\infty \exp(-st)f(t)dt, \quad (35)$$

let  $\tilde{V}(s) \equiv \mathcal{L}\langle v_x^{(2)} \rangle$ , and  $\tilde{\Theta}(s) \equiv \mathcal{L}\langle \theta^{(2)} \rangle$ . Then

$$\tilde{V}'' + \frac{1}{2Er} \tilde{\Theta}''' = 0 \quad (36)$$

$$s\tilde{\Theta} - \frac{1}{Er} \frac{\mu}{\gamma} \tilde{\Theta}'' + \frac{1}{2} \tilde{V}' = -\tilde{g}, \quad (37)$$

where  $\tilde{g} = g/s$  and the primes denote differentiation with respect to  $y$ . Note that (36) and the fact that  $\theta^{(2)}$  and  $v_x^{(2)}$  are finite at  $y \rightarrow \infty$  implies that  $\tilde{V}' + \tilde{\Theta}''/2/Er$  is a constant. Thus, (37) becomes diffusion with a source,

$$s\tilde{\Theta} - D\tilde{\Theta}'' = -\tilde{g}, \quad (38)$$

where the diffusion constant is

$$D = \frac{1}{Er} \left( \frac{\mu}{\gamma} + \frac{1}{4} \right). \quad (39)$$

The solution is

$$\begin{aligned} \tilde{\Theta} &= \frac{\epsilon^2}{2s} \frac{s - 12D}{(s - 4D)^2} e^{-y\sqrt{s/D}} \\ &+ \frac{\epsilon^2}{2s} \frac{12D - s + (8D - 2s)y}{(s - 4D)^2} e^{-2y}. \end{aligned} \quad (40)$$

Note that we recover the proper long-time limit of the second-order angle field in steady-state swimming [23]:

$$\lim_{s \rightarrow 0} s\tilde{\Theta} = \epsilon^2 \frac{\gamma Er}{2(4\mu + \gamma)} [(3 + 2y)e^{-2y} - 3]. \quad (41)$$

The angle field  $\tilde{\Theta}$  has an explicit inverse Laplace transform:

$$\begin{aligned} \langle \theta^{(2)} \rangle &= \frac{\epsilon^2}{16D} \left\{ (6 + 4y) e^{-2y} - 6 \operatorname{erfc} \left[ y/(2\sqrt{Dt}) \right] \right. \\ &+ (8Dt - 3 - 2y) \\ &\times \left. \left[ e^{4Dt-2y} \operatorname{erfc}(z_-) - e^{2y} \operatorname{erfc}(z_+) \right] \right\}, \end{aligned} \quad (42)$$

where  $\operatorname{erfc}$  is the complementary error function [25], and

$$z_\pm \equiv \frac{4Dt \pm y}{2\sqrt{Dt}}. \quad (43)$$

Note that since  $D \propto 1/Er$ , we have  $\langle \theta^{(2)} \rangle \propto Er$ . Figure 2 shows how  $\langle \theta^{(2)} \rangle$  evolves to its final steady-state value. Note that for any finite  $t$ , the second-order angle field vanishes at  $y \rightarrow \infty$ . However, for a given  $y \gtrsim 1$ , we can always wait long enough for the angle field to reach its steady-state value of  $-3\epsilon^2\gamma Er/(8\mu + \gamma)$ . Despite the complicated form of Eq. (42), close examination of the plots of  $\langle \theta^{(2)} \rangle$  for various  $t$  (Fig. 2) reveals that the  $y$ -value at which  $|\langle \theta^{(2)} \rangle|$  attains half its maximum value increases like  $t^{1/2}$ , as expected for diffusion.

We can also solve for the velocity field in Laplace space:

$$\tilde{V} = v_1 e^{-y\sqrt{s/D}} + v_2 e^{-2y} + \tilde{U}, \quad (44)$$

where

$$v_1 = \epsilon^2 \frac{\sqrt{s^3/D} - 12\sqrt{s/D}}{4Er s (s - 4D)^2} \quad (45)$$

$$v_2 = \epsilon^2 \frac{-4sy + 16D(1 + y)}{4Er s (s - 4D)^2}, \quad (46)$$

and the term  $\tilde{U}$  remaining in the limit  $y \rightarrow \infty$  is the swimming speed in the frequency domain,

$$\tilde{U} = \left[ \frac{1}{2s} - \frac{4 + \sqrt{s/D}}{sEr(2\sqrt{D} + \sqrt{s})^2} \right] \epsilon^2. \quad (47)$$

Note that the long-time limit of the swimming speed agrees with the steady-state result [23]:

$$\lim_{s \rightarrow 0} s\tilde{U} = U_\infty = \frac{\epsilon^2}{2} \frac{4\mu - \gamma}{4\mu + \gamma}. \quad (48)$$

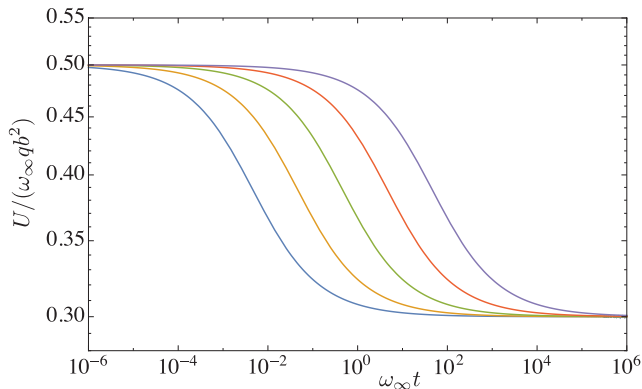


Figure 3. (Color online) Dimensionless swimming speed vs dimensionless time on a log-log scale for  $\mu = \gamma$  and Er ranging from (from left to right) Er= 0.01 (blue), Er=0.1 (gold), Er=1 (green), Er= 10 (red), and Er= 100 (purple).

By inspection of  $\tilde{\Theta}$ ,  $\tilde{V}$ , and  $\tilde{U}$ , we observe that the characteristic time scale for disturbances to diffuse over a distance  $L$  is  $L/\sqrt{D} \propto L\sqrt{\text{Er}\gamma/(\mu + \gamma/4)}$ .

We were unable to find an analytic form for the velocity field in the time domain. However, we can solve for the swimming speed in the time domain by integrating Eq. (36) in the time domain with respect to  $y$ . Let  $V = \langle v_x^{(2)} \rangle$  and  $\Theta = \langle \theta^{(2)} \rangle$ . One integration yields  $V' + \Theta''/(2\text{Er}) = 0$ , since all  $y$ -derivatives of  $V$  and  $\Theta$  must vanish at  $y \rightarrow \infty$ . One more integration shows that  $V + \Theta'/(2\text{Er})$  is constant; this constant must equal the flow speed at  $y \rightarrow \infty$ , again because  $\Theta'$  vanishes at  $y \rightarrow \infty$ . Thus,

$$U = V(y, t) + \frac{1}{2\text{Er}} \frac{\partial \Theta}{\partial y}(y, t). \quad (49)$$

But  $V(0, t) = \epsilon^2/2$ ; therefore

$$U = \frac{\epsilon^2}{2} + \frac{1}{2\text{Er}} \partial_y \Theta \Big|_{y=0}. \quad (50)$$

Substituting Eq. (42) into (50) yields

$$U = U_\infty + U_{\text{tr}}, \quad (51)$$

where

$$U_\infty = \frac{1}{2} - \frac{1}{4D\text{Er}} = \frac{1}{2} \frac{4\mu - \gamma}{4\mu + \gamma} \quad (52)$$

is the steady-state speed at  $t \rightarrow \infty$  [23], and

$$U_{\text{tr}} = \epsilon^2 \left[ \frac{1}{2\text{Er}} \sqrt{\frac{t}{D\pi}} + \frac{1}{\text{Er}} \left( \frac{1}{4D} - t \right) e^{4Dt} \text{erfc} \left( 2\sqrt{Dt} \right) \right] \quad (53)$$

is a transient contribution that decays for large  $t$  as

$$U_{\text{tr}} \sim \frac{3}{16(\mu/\gamma + 1/4)^{3/2}} \sqrt{\frac{\text{Er}}{\pi t}} + \mathcal{O}(1/t^{3/2}). \quad (54)$$

The evolution of the swimming speed in time for various Er is shown in Fig. 3. Since the curves in Fig. 3 are equally spaced in  $\log(\text{Er})$  and are also equally spaced on the log-log plot, the time to reach the midway point between  $\omega_\infty q b^2/2$  and  $U_\infty$  increases linearly with Er. We can also see that the time to reach the steady state increases linearly with Er from Eq. (54): the dimensionless time  $t^*$  it takes  $U_{\text{tr}}$  to decay to a small fraction of the steady-state speed is

$$t^* \propto \frac{\text{Er}}{(\mu/\gamma + 1/4)^3}. \quad (55)$$

Note that  $t^* \propto \text{Er}(\gamma/\mu)^3$  for  $\gamma \ll \mu$ , and  $t^* \propto \text{Er}$  for  $\gamma \gg \mu$ .

#### IV. ARBITRARY ANCHORING STRENGTH

We now turn to the swimming problem with finite but arbitrary anchoring strength  $w$ . Again we work in powers of the dimensionless amplitude  $\epsilon$ . To first order we can find an analytic form for the Laplace transforms of the angle field and stream function. At second order we consider limits such as large Ericksen number, small Ericksen number, and vanishing anchoring strength.

##### A. First-order swimming problem

To write the Laplace transform of the governing equations (8–9) to first order in  $\epsilon$ , we need to find the initial value of the angle field, since  $\mathcal{L}\{\partial_t \theta^{(1)}\} = -\theta^{(1)}(t=0) + s\mathcal{L}\{\theta^{(1)}\}$ . The initial condition for the angle field is that it is the equilibrium field obeying the anchoring condition (6) for the initial swimmer shape,  $y_m = -i \exp ix$  in complex notation, which leads to

$$0 = \nabla^4 \tilde{\psi}^{(1)} + \frac{1}{2\text{Er}} \nabla^4 \tilde{\theta}^{(1)} \quad (56)$$

$$s\tilde{\theta}^{(1)} = \frac{\mu}{\gamma\text{Er}} \nabla^2 \tilde{\theta}^{(1)} - \frac{1}{2} \nabla^2 \tilde{\psi}^{(1)} + \frac{w\epsilon}{1+w} e^{ix-y}. \quad (57)$$

The solutions to Eqns. (56–57) are

$$\tilde{\psi}^{(1)} = (c_0 + c_1 y) e^{-y+ix} - \frac{1}{2\text{Er}} \tilde{\theta}^{(1)} \quad (58)$$

$$\tilde{\theta}^{(1)} = \left[ \frac{1}{s} \left( c_1 + \frac{w\epsilon}{1+w} \right) e^{-y} + c_2 e^{ky} \right] e^{ix}, \quad (59)$$

where

$$k = -\sqrt{1 + \frac{4s\gamma\text{Er}}{\gamma + 4\mu}}, \quad (60)$$

and the  $s$ -dependent coefficients  $c_0$ ,  $c_1$ , and  $c_2$  are determined by the no-slip and anchoring boundary conditions at the surface of the swimmer. In Laplace space, the no-slip boundary condition  $\mathbf{v}(x_m, y_m) = (x_m, \partial_t y_m)$  becomes

$$\left(\partial_y \tilde{\psi}^{(1)}, -\partial_x \tilde{\psi}^{(1)}\right)\Big|_{y=0} = \left(0, -\epsilon \frac{e^{ix}}{i+s}\right) \quad (61)$$

to first order in dimensionless form. Likewise, to first order, the anchoring boundary condition (13) becomes

$$-\partial_y \tilde{\theta}^{(1)}\Big|_{y=0} + w \left(\tilde{\theta}^{(1)}\Big|_{y=0} - \epsilon \frac{e^{ix}}{i+s}\right) = 0. \quad (62)$$

Although analytic expressions for  $c_0$ ,  $c_1$ , and  $c_2$  and also  $\tilde{\psi}^{(1)}$  and  $\tilde{\theta}^{(1)}$  can be computed for arbitrary  $w$ , their lengthy form prevents us from displaying them here. In the next two subsections we consider the limits of large and small Ericksen number. Just as in the strong anchoring case and the sinusoidal steady-state case [23], there is no swimming speed to first order.

## B. Asymptotic solution at high Ericksen number

Our analysis in the limit of  $\text{Er} \gg 1$  is similar to that in the sinusoidal steady-state problem [23]. Expanding the coefficients from the first-order problem to leading order in inverse powers of Ericksen number, we find

$$c_0 = -\frac{i\epsilon}{i+s} + \mathcal{O}\left(\frac{1}{\text{Er}}\right) \quad (63)$$

$$c_1 = -\frac{i\epsilon}{i+s} + \mathcal{O}\left(\frac{1}{\text{Er}}\right) \quad (64)$$

$$c_2 = \frac{1}{\sqrt{\text{Er}}} \frac{i\epsilon\sqrt{1/4 + \mu/\gamma}}{(i+s)\sqrt{s^3}} + \mathcal{O}\left(\frac{1}{\text{Er}}\right) \quad (65)$$

With an accuracy of  $\mathcal{O}(1/\sqrt{\text{Er}})$ , the coefficients  $c_0$ ,  $c_1$ , and  $c_2$  are independent of the anchoring strength, and take the same values as in the strong-anchoring problem; the rapidly varying component, proportional to  $\exp ky$ , which does not arise in the strong-anchoring limit, has an amplitude of  $\mathcal{O}(1/\sqrt{\text{Er}})$ . Thus we conclude that the first-order flow field and angle field at large Ericksen number and *arbitrary* anchoring is well-approximated by the solutions to the *strong*-anchoring problem.

The second-order flow and angle field at large Ericksen number and arbitrary anchoring strength is also given by the strong-anchoring solutions. To see why, note that large  $\text{Er}$ , the second-order equations (29–30) are identical to the strong-anchoring equations since  $f$  and  $g$  depend only on first-order quantities. For arbitrary  $w$ , the boundary conditions at second order are

$$\langle v_x^{(2)} \rangle = -\langle y_m \partial_y v_x^{(1)} \rangle \quad (66)$$

and

$$\begin{aligned} &\langle -\partial_y \theta^{(2)} + w \theta^{(2)} \rangle_{y=0} \\ &= \langle -\partial_x y_m \partial_x \theta^{(1)} + y_m \partial_y^2 \theta^{(1)} - w y_m \partial_y \theta^{(1)} \rangle_{y=0}. \end{aligned} \quad (67)$$

The terms on the right-hand sides of (66–67) arise from expanding the boundary about  $y = 0$ , and depend on the anchoring strength  $w$  implicitly through the first-order quantities. However, for large  $\text{Er}$  these quantities are given by the strong-anchoring limit; in particular, all the terms on the right-hand side of (67) vanish since  $y_m$  and  $\theta^{(1)}$  are out of phase for strong anchoring. Furthermore, the value of  $\partial_y \theta^{(2)}$  at  $y = 0$  is  $\mathcal{O}(\sqrt{\text{Er}})$ . Since the angle field  $\theta^{(2)}$  is  $\mathcal{O}(\text{Er})$  [see Eq. (42)], the term  $\langle \partial_y \theta^{(2)} \rangle_{y=0}$  is subleading in  $\text{Er}$ . Therefore, large  $\text{Er}$  behavior of the arbitrary anchoring strength problem is the strong-anchoring problem. The steady-state angle field evolves slowly, with a characteristic time proportional to  $\text{Er}$ .

## C. Asymptotic solution for low Ericksen number

In this section we show explicitly for arbitrary dimensionless anchoring strength  $w$  that the angle field attains its steady-state value quickly when the Ericksen number is low, with a startup time proportional to  $\text{Er}$ . Consider the governing equations (3) and (4) in the limit of  $\text{Er} \ll 1$ . In this limit the viscous stresses are weak compared to elastic stresses. Note that sending  $\text{Er}$  to zero removes the highest (and only) time derivative in Eq. (4). Therefore, we have a singular perturbation theory problem, with an inner problem for early time and an outer problem for late time. The outer problem is the steady-state problem studied in [23]. We introduce the short time scale  $\tau = t \text{Er}$  to resolve the fast relaxation of the angle field and flow to their steady-state values. Thus, we formally expand the fields at each order of  $\epsilon$  in powers of  $\text{Er}$ . For example,  $\psi^{(1)}(t, \text{Er}) = \psi_0^{(1)}(t, \tau) + \text{Er} \psi_1^{(1)}(t, \tau) + \dots$ . Note that

$$\partial_t \theta^{(1)} = \frac{1}{\text{Er}} \partial_\tau \theta_0^{(1)} + \partial_t \theta_0^{(1)} + \partial_\tau \theta_1^{(1)} + \dots \quad (68)$$

Only the angle field enters the zeroth order equations:

$$\nabla^4 \theta_0^{(1)} = 0 \quad (69)$$

$$\partial_\tau \theta_0^{(1)} = \frac{\mu}{\gamma} \nabla^2 \theta_0^{(1)}. \quad (70)$$

Expanding the boundary condition in  $\text{Er}$  leads to

$$w(\theta_0^{(1)}\Big|_{y=0} - \epsilon \cos(x)) = \partial_y \theta_0^{(1)}\Big|_{y=0}. \quad (71)$$

To zeroth order in  $\text{Er}$ , the solution is

$$\theta_0^{(1)} = \epsilon \frac{w}{1+w} e^{-y} \cos x. \quad (72)$$

Note that since the wave of the swimmer is stationary

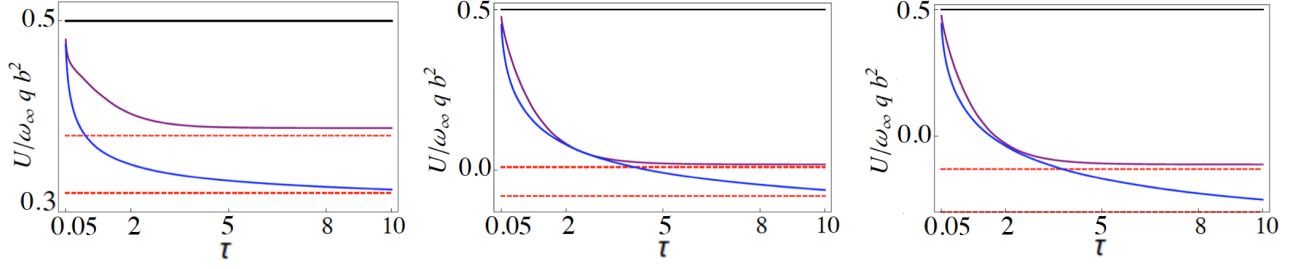


Figure 4. (Color online) Plots of the dimensionless swimming speed  $U/(\omega_\infty q b^2)$  vs.  $\tau$  for  $\text{Er} \ll 1$  and  $\log(\gamma/\mu) = 0$  (left panel),  $\log(\gamma/\mu) = 1$  (middle panel), and  $\log(\gamma/\mu) = 3$  (right panel). Colors correspond to  $w = 0.001$  (black),  $w = 1$  (purple), and  $w = 1000$  (blue). Red dashed lines indicate the steady swimming speed found in [23].

on the fast time scale  $\tau$ , the angle field is simply the equilibrium angle field for a stationary ripple.

Turning now to the next order in  $\text{Er}$ , we have

$$\nabla^4 \psi_0^{(1)} + \frac{1}{2} \nabla^4 \theta_1^{(1)} = 0 \quad (73)$$

$$\partial_\tau \theta_1^{(1)} + \frac{1}{2} \nabla^2 \psi_0^{(1)} = \frac{\mu}{\gamma} \nabla^2 \theta_1^{(1)}, \quad (74)$$

with boundary conditions

$$(\partial_y \psi_0^{(1)}, -\partial_x \psi_0^{(1)})_{y=0} - (0, -\epsilon \cos x) = 0 \quad (75)$$

$$\left[ w(\theta_1^{(1)} - \epsilon \tau \sin x) - \partial_y \theta_1^{(1)} \right]_{y=0} = 0 \quad (76)$$

and initial conditions  $\psi_0^{(1)} = 0$  and  $\theta_1^{(1)} = 0$ . The form of Eqs. (73–74) is similar to the form of (56–57), and the Laplace transforms of  $\psi_0^{(1)}$  and  $\theta_1^{(1)}$  are readily found. However, we are not able to find an explicitly analytic expression for the inverse Laplace transform of these quantities. The boundary conditions (75–76) and the governing equations (73–74) imply  $\psi_0^{(1)} \propto \sin x$  and  $\theta_1^{(1)} \propto \sin x$ . These phase relations apply because the swimmer wave is stationary on the small timescale  $t \text{Er}$  over which the fields develop from their initial values.

Now consider the problem to second order in  $\epsilon$ . To zeroth order in  $\text{Er}$ , the second-order problem is

$$\begin{aligned} \partial_y^3 \langle \theta_0^{(2)} \rangle &= 0 \\ \partial_\tau \langle \theta_0^{(2)} \rangle &= \frac{\mu}{\gamma} \partial_y^2 \langle \theta_0^{(2)} \rangle, \end{aligned} \quad (77)$$

suggesting that  $\langle \theta_0^{(2)} \rangle$  is a constant. The boundary condition at this order is

$$\left[ -\langle \partial_y \theta_0^{(2)} \rangle + w \langle \theta_0^{(2)} \rangle \right]_{y=0} = 0, \quad (78)$$

implying  $\langle \theta_0^{(2)} \rangle = 0$ .

To first order in  $\text{Er}$ , we have

$$\begin{aligned} \partial_y^2 \langle v_{x0}^{(2)} \rangle + \frac{1}{2} \partial_y^3 \langle \theta_1^{(2)} \rangle &= \langle \partial_x \theta_0^{(1)} \nabla^2 \theta_1^{(1)} \rangle \\ \partial_\tau \langle \theta_1^{(2)} \rangle + \frac{1}{2} \partial_y \langle v_{x0}^{(2)} \rangle &= \frac{\mu}{\gamma} \partial_y^2 \langle \theta_1^{(2)} \rangle - \langle v_0^{(1)} \cdot \nabla \theta_0^{(1)} \rangle. \end{aligned} \quad (79)$$

The boundary conditions to second order in  $\epsilon$  and first order in  $\text{Er}$  are greatly simplified by the observation that  $\theta_1^{(1)}$  and  $y_m$  are in phase in  $x$ , which makes many terms vanish when we expand  $y_m$  to first order in  $\text{Er}$ ,  $y_m = \epsilon \sin x - \epsilon \text{Er} \tau \cos x$ . Thus

$$\langle v_{x0}^{(2)} \rangle|_{y=0} = -\epsilon \langle \partial_y v_{x0}^{(1)} \sin x \rangle \quad (80)$$

$$\left[ -\langle \partial_y \theta_1^{(2)} \rangle + w \langle \theta_1^{(2)} \rangle \right]_{y=0} = 0 \quad (81)$$

Since  $\theta_0^{(1)}$  is independent of time, it is straightforward to analytically determine the Laplace transform Eq. (79). Using the boundary condition (81) to determine the Laplace transform of  $\langle \theta_1^{(2)} \rangle$ , we may use the same methods as in Section III to solve for the swimming speed  $\tilde{U}(s)$ . We could not find an exact inverse Laplace transform for this function except in the limit  $w \rightarrow \infty$ , so we invert the expression numerically using a Fourier/de Hoog type method [26] on the interval  $t/\tau \in [0.05, 20]$  with 2,048 gridpoints. Figure 4 shows that the swimming speed relaxes to the steady state value with a characteristic time proportional to  $\text{Er}$  for various anchoring strengths.

#### D. Zero anchoring

The final limit we consider is zero anchoring strength,  $w = 0$ , for arbitrary Ericksen number. We proceed as above, by solving the governing equations to first order in  $\epsilon$  analytically using the Laplace transform, finding the angle field and swimming velocity in the frequency domain to second order in  $\epsilon$ , and then using the Fourier/de Hoog method to invert the Laplace transform to find the swimming speed  $U(t)$ . The results are shown in Fig. 5 for  $\text{Er}=1$ . When  $\gamma/\mu$  is sufficiently small, less than around 10, the ultimate swimming direction is opposite the direc-

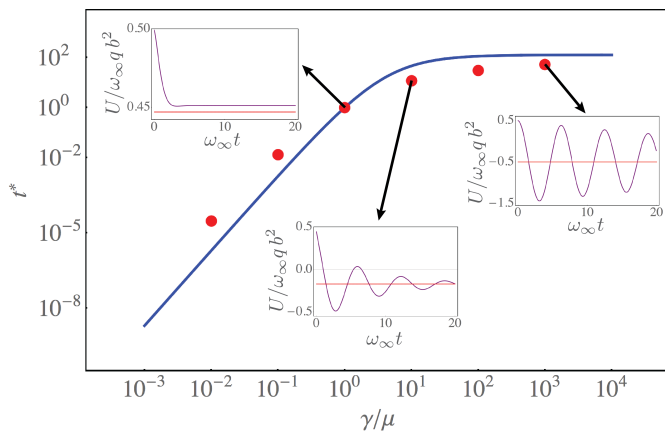


Figure 5. (Color online) Log-log plot of the dimensionless time  $t^*$  to attain the steady-state swimming speed versus  $\gamma/\mu$  for  $Er = 1$ . The time  $t^*$  is defined to be the time in which the amplitude of the envelop of the oscillations (if there are any) is 5% of the ultimate swimming speed. The red dots are the values of  $t^*$  for zero anchoring strength,  $w = 0$ . For comparison, the solid blue line corresponds to the case of strong anchoring. To best compare the dependence of  $\gamma/\mu$ , the time-origins of both graphs have been shifted by defining  $t^* = 1$  for  $\gamma = \mu$ . The insets show the numerically computed swimming speeds versus dimensionless time for  $\gamma/\mu = 1, 10, \text{ and } 1000$ .

tion of the traveling waves of the stroke [23]. When  $\gamma/\mu$  is large enough, the swimmer ultimately swims in the same direction as the traveling waves. Figure 5 shows that in these cases the swimming speed oscillates about the final swimming speed as the steady state develops; when  $\gamma/\mu$  is large there can be several time intervals in which the

swimmer changes direction before it settles down into its steady swimming speed.

## V. CONCLUSION

In conclusion, we have studied the time-evolution of a swimmer in a hexatic liquid crystal film. The swimmer in our approximation has a small amplitude sinusoidal stroke that begins abruptly. Since the startup of viscous flow is much faster than the evolution of the liquid crystal configuration, the swimmer immediately begins swimming with the Newtonian swimming speed. It reaches the ultimate steady-state swimming speed with a dimensionless characteristic time that is proportional to the Ericksen number, or, equivalently, a characteristic time proportional to  $\mu/(Kq^2)$ . When the Ericksen number is large, the behavior is independent of that anchoring strength and given by the limit of infinite anchoring. When the anchoring strength vanishes, the transient swimming speed can oscillate, and even change sign. Although the high symmetry of a hexatic liquid crystal lead to great simplifications in our analysis, we expect that many of the phenomena we found here will serve as a guide for the investigation of more the more realistic but complicated case of a finite-size swimmer in a three-dimensional nematic liquid crystal.

## ACKNOWLEDGMENTS

This work was supported in part by National Science Foundation Grant Nos. CBET-1437195 (TRP) and CBET-1336638 (TRP).

- 
- [1] E. Lauga and T. R. Powers. The hydrodynamics of swimming microorganisms. *Rep. Prog. Phys.*, **72**:096601, 2009.
  - [2] D. A. Gagnon, N. C. Keim, and P. E. Arratia. Undulatory swimming in shear-thinning fluids: experiments with *Caenorhabditis elegans*. *J. Fluid Mech.*, **758**:R3, 2014.
  - [3] M. Molaei, M. Barry, R. Stocker, and J. Sheng. Failed escape: solid surfaces prevent tumbling of *Escherichia coli*. *Phys. Rev. Lett.*, **113**:068103, 2014.
  - [4] J. Li, S. Sattayasamitsathit, R. Dong, W. Gao, R. Tam, X. Feng, S. Ai, and J. Wang. Template electrosynthesis of tailored-made helical nanoswimmers. *Nanoscale*, **6**:9415, 2014.
  - [5] B. J. Williams, S. V. Anand, J. Rajagopalan, and M. T. A. Saif. A self-propelled biohybrid swimmer at low Reynolds number. *Nat. Commun.*, **5**:3081, 2014.
  - [6] Y. Magariyama, S. Sugiyama, K. Muramoto, I. Kawagishi, Y. Imae, and S. Kudo. Simultaneous measurement of bacterial flagellar rotation rate and swimming speed. *Biophys. J.*, **69**:2154, 1995.
  - [7] H. C. Berg. The rotary motor of bacterial flagella. *Ann. Rev. Biochem.*, **72**:19–54, 2003.
  - [8] R. Kamiya and E. Hasegawa. Intrinsic difference in beat frequency between the two flagella of *Chlamydomonas reinhardtii*. *Exp. Cell Res.*, **173**:299, 1987.
  - [9] B. H. Gibbons and I. R. Gibbons. Flagellar movement and adenosine triphosphatase activity in sea urchin sperm extracted with Triton X-100. *J. Cell Biol.*, **54**:75, 1972.
  - [10] D. J. Smith, E. A. Gaffney, H. Gadêlha, N. Kapur, and J. C. Kirkman-Brown. Bend propagation in the flagella of migrating human sperm, and its modulation by viscosity. *Cell Mot. Cytos.*, **66**:220, 2009.
  - [11] X. N. Shen and P. E. Arratia. Undulatory swimming in viscoelastic fluids. *Phys. Rev. Lett.*, **106**:208101, 2011.
  - [12] O. S. Pak and E. Lauga. The transient swimming of a waving sheet. *Proc. Roy. Soc.*, **466**:107, 2010.
  - [13] B. Liu, T. R. Powers, and K. S. Breuer. Force-free swimming of a model helical flagellum in viscoelastic fluids. *Proc. Natl. Acad. Sci. (USA)*, **108**:19516, 2011.
  - [14] A. Gilboa and A. Silberberg. In situ rheological characterization of epithelial mucus. *Biorheology*, **13**:59, 1976.
  - [15] S. K. Lai, Y.-Y. Wang, D. Wirtz, and J. Hanes. Micro-

- and macrorheology of mucus. *Adv. Drug Deliv. Rev.*, **6**:86, 2009.
- [16] G. J. Elfring and E. Lauga. Theory of locomotion through complex fluids. In S. E. Spagnolie, editor, *Complex fluids in biological systems*. Springer, Berlin, 2015.
- [17] S. Zhou, A. Sokolov, O. D. Lavrentovich, and I. S. Aranson. Living liquid crystals. *Proc. Natl. Acad. Sci. USA*, **111**:1265, 2014.
- [18] P. C. Mushenheim, R. R. Trivedi, H. H. Tuson, D. B. Weibel, and N. L. Abbott. Dynamic self-assembly of motile bacteria in liquid crystals. *Soft Matter*, **10**:88, 2014.
- [19] G. I. Taylor. Analysis of the swimming of microscopic organisms. *Proc. R. Soc. Lond. Ser. A*, **209**:447–461, 1951.
- [20] L. Xie, T. Altindal, S. Chattopadhyay, and X.-L. Wu. Bacterial flagellum as a propeller and as a rudder for efficient chemotaxis. *Proc. Natl. Acad. Sci. USA*, **108**:2246, 2011.
- [21] S. F. Goldstein. Starting transients in sea urchin sperm flagella. *J. Cell Biol.*, **80**:61, 1979.
- [22] P. G. de Gennes and J. Prost. *The Physics of Liquid Crystals*. Oxford University Press, Oxford, 2nd edition, 1995.
- [23] M. S. Krieger, S. E. Spagnolie, and T. R. Powers. Locomotion and transport in a hexatic liquid crystal. *Phys. Rev. E*, **90**:052503, 2014.
- [24] L. D. Landau and E. M. Lifshitz. *Theory of elasticity*. Pergamon Press, Oxford, 3rd edition, 1986.
- [25] M. Abramowitz and I. A. Stegun. *Handbook of Mathematical Functions*. Dover Publications, Inc., New York, 1964.
- [26] B. Davies and B. Martin. Numerical inversion of the laplace transform: a survey and comparison of methods. *J. Comp. Physics*, **33**:1–32, 1979.